JETIR.ORG ISSN: 2349-5162 | ESTD Year : 2014 | Monthly Issue
JOURNAL OF EMERGING TECHNOLOGIES AND INNOVATIVE RESEARCH (JETIR)
An International Scholarly Open Access, Peer-reviewed, Refereed Journal

Experimental and Computational Analysis of Tracking Phenomenon in Polymeric Insulator using Comparative Tracking Index Test

[1]Chintan Patel, [2]R R Patel

[1]DResearch Scholar, Gujarat Technological University, Ahmedabad, [2]Professor
[1,2]Department of Electrical Engineering, G H Patel College of Engineering & Technology,
Vallabh Vidyanagar, Gujarat, India

Abstract : Due to their superior electrical, mechanical, and thermal qualities, polymeric (silicon rubber) insulators are frequently chosen in overhead transmission networks. To increase the dependability of the insulators, it is critical to comprehend the distinct features of such materials. The Comparative Tracking Index (CTI) test is used in the current study to examine the surface characteristics and process of deterioration caused by electrical stress in the presence of contaminants. Because of dry band arcing on the sample's surface, it is discovered that the contaminants have a significant impact on the surface conditions of the material, leading to tracking, degradation, and mass erosion. Additionally, the CTI test is simulated using the COMSOL Multiphysics software, which showed that the concentration of the electric field is increased between the electrodes, which can cause the material to degrade and ultimately fail.

Index Terms **- Polymeric Insulator, Surface Degradation, Erosion, Comparative Tracking Index, Electric Field.**

I. INTRODUCTION

Polymeric insulators (silicon rubber) are very popular as electrical insulating material in outdoor applications like power transmission network because of their superior performance over conventional materials. They are light in weight, flexible to handle, and possess excellent hydrophobicity. However, the material suffers from degradation due to various factors like electrical stresses, UV radiations, industrial pollutants, etc. Failure of insulation can result in the damage of any electrical equipment and hence the reliability of the power system operation strongly depends on the insulation [1,2,3]. The surface properties of the material play an important role when it is used in overhead transmission systems. The performance of the polymeric insulator is greatly affected by environmental factors like fog, dust, mist, moisture, and pollutants. Loss of molecular weight due to surface erosion is one of the key issues for the failure of the insulator. To study the loss of material properties due to aging, the assessment of resistance to tracking and erosion is one of the essential analyses [4]. Failure due to surface tracking occurs because of a polluted and wet surface, dry-band arcing due to joule heat, carbonization on the surface due to the partial discharge, propagation of the carbonization, and formation of tracks [5].

The experimental study had been carried out on polymeric insulators with the comparative tracking index (CTI) experiments as per IEC-60112 (2003). They analysed the effects of electrolyte composition and electrode materials and revealed that the solution with higher conductivity reduces the CTI value and performance of the material is degraded [6,7]. The relationship between tracking phenomena and the performance of dispersed metals has been studied from various electrodes like Copper, Brass, and Platinum at the interface between electrolytic material and paper phenolic laminate [8]. The association between the discharge energy and tracking resistance was examined by researchers. The results show that the tracking resistances of the samples change with gamma-ray irradiation [9,10,11]. The study of the surface erosion on polymeric insulating material using CTI experimentation as per IEC60112 with the help of the Fourier transform infra-red (FTIR) analysis and Scanning Electron Microscopy (SEM) to evaluate the surface erosion of the samples due to electrical stress revealed a useful information about surface degradation of the material [12]. The investigation of the tracking phenomenon in cable joints using the finite element method was done using the 3D model of the CTI test experiment and the effect of contaminant droplets had been analysed. The authors found that the presence of droplets between the electrode greatly affects the tracking on the surface of the material [13]. The burn-in patterns on solid elastic insulating material had been examined using the CTI test. The burn-in patterns observed were the result of current density maxima between the electrodes [14]. CTI test was performed to examine the surface properties of nanocomposites. The authors concluded that the samples with better hydrophobicity exhibited a higher tracking resistance [15].

In this study, tracking phenomena on the surface of the silicon rubber is investigated with the help of the CTI experiment method as per IEC60112 and finite element method using COMSOL Multiphysics. Electric potential and electric field distribution on the surface of the silicon rubber between electrodes were simulated for various positions of the contaminant droplets. For experimental analysis, the test samples were cut from the virgin and aged insulating material as per the dimensions specified by the

standard. The aged insulating material was received from a local power distribution company. With the help of the CTI experiment, the effect of several droplets and voltage magnitude on the surface tracking has been studied to understand the surface degradation of the material. Further, the surface condition is analysed with the help of digital image processing by edge detection in MATLAB.

II. Materials and Methods

2.1. CTI Test

The standard test set-up is prepared to study the relative resistance of solid insulation materials to tracking using AC supply voltages using IEC 60112 [7]. Fig. 1 shows the experimental test set-up for tracking and erosion. It consists of two chisel-shaped electrodes put on an insulating material sample to be tested with a gap distance of 4 mm between the electrodes.

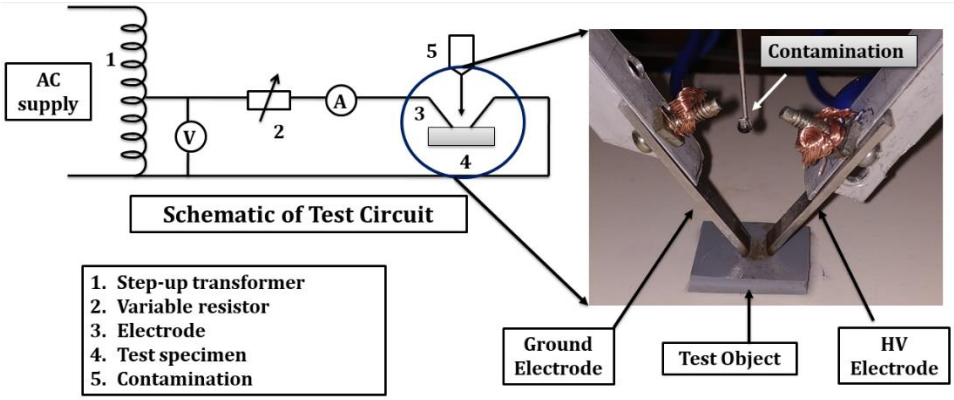

Figure 1 Experimental Set-up for Surface Erosion Study

An autotransformer of 0-240 V was used to apply the voltage to the electrodes. A rheostat was placed in the circuit to limit the short circuit current. The purpose of the CTI test was to study the surface tracking performance of the polymer insulating material under polluted and moist conditions. The solution consisting of 0.1% NH4Cl (ammonium chloride) was allowed to drop, with a volume of 20 ± 5 mm3, at an interval of 30 ± 5 seconds on the sample surface to mimic the environmental conditions [7]. The needle was set such that the droplet falls in the middle of the electrodes. According to the test standards, electrodes with 2 mm thickness and 5 mm width were mounted on the support. The dimensions of the test samples were 20 mm2 × 20 mm2 and the width of the sample was 3 mm [16]. The electrodes were mounted in such a way that they were in contact of the sample surface horizontally at an angle of 60°.

2.2. Edge Detection

On the images of the tested materials, the Sobel and Prewitt edge detection algorithms were used in MATLAB to count the number of edges that denote surface erosion. [17,18]. The methods operate by identifying the gradient of image intensity at each image pixel. It aids in distinguishing between each pixel's darker and brighter values. The edge detection is carried out by following the given steps:

1) Read the image.
2) Convert into grayscale if it is RGB image.
3) Convert the image into the double format.
4) Define the suitable mask or filter (Sobel or Prewitt).
5) Detect the edges along X-axis.
6) Detect the edges along Y-axis.
7) Combine the edges detected along the X and Y axes.
8) Display all the images.

When applied to an image, the Sobel operator allows quick execution while also producing the same result (without changing the original image). It is a 3 x 3 convolution kernel that employs two 3 x 3 size masks, one to estimate the gradient in the X-direction and the other for the gradient's Y-direction. For obtaining gradient components in each direction, the kernel can be applied separately to each orientation of the input image. Calculations are made to determine the edge's size or strength using equation (1)

-1	0	+1	+1	+2	+1
-2	0	+2	0	0	0
-1	0	+1	-1	-2	-1
Gx-Horizontal			Gy-Vertical		

Table 1: Mask Filter for Sobel Algorithm

$$|G| = \sqrt{G_x^2} + \sqrt{G_y^2} \qquad (1)$$

In the case of the Prewitt algorithm, the following mask filter is used to sense the edges (given in Table 2). The remaining process to count the edges is the same as the Sobel algorithm.

-1	0	+1	+1	+1	+1
-1	0	+1	0	0	0
-1	0	+1	-1	-1	-1
Gx-Horizontal			Gy-Vertical		

Table 1: Mask Filter for Prewitt Algorithm

2.3. Modelling of CTI Test

The CTI test configuration is modelled with COMSOL Multiphysics software based on the finite element method [19]. The sample and electrode assembly were modelled in 3D with the specified dimensions. The 3D geometry compliant with IEC 60112 test standards is shown in Figure 2.

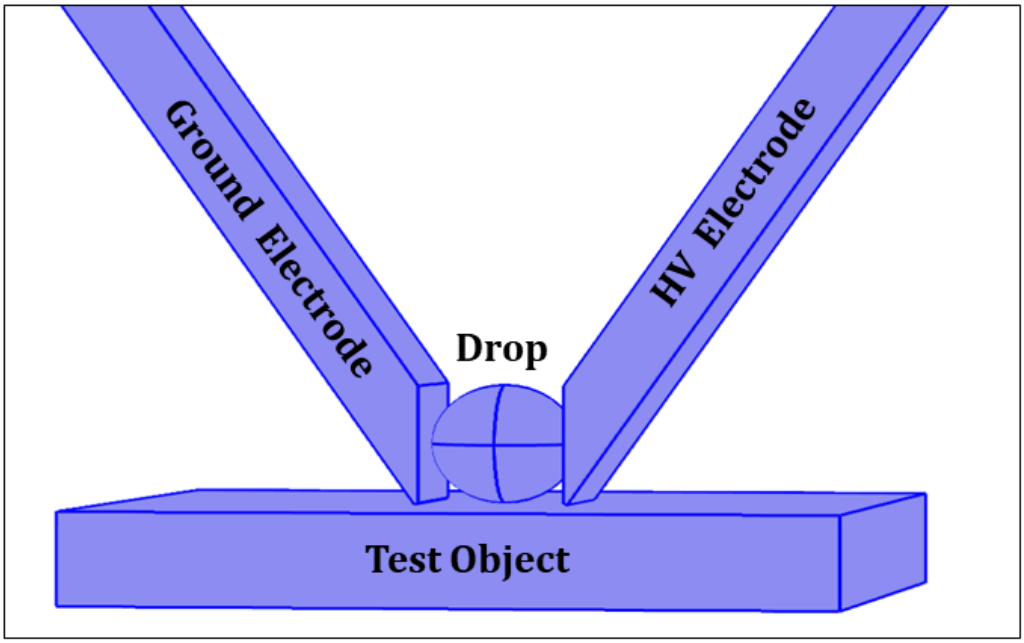

Figure 2: 3D Model of CTI Test

After the model geometry was prepared, the materials of the CTI experiment set are defined for test sample (silicon rubber), electrodes (steel), and droplet (water) with the properties as specified in Table 3.

Table 3: Properties of Materials used in Simulation

Geometry	Material	Relative Permittivity (ε_r)	Conductivity (S/m)
Test Object	Silicon Rubber (SR)	4.2	10^{-12}
Electrodes	Steel	1	4.032×10^{6}
Droplet	Water	80	0.25

An electric potential of 400 V was applied to the HV electrode whereas the other electrode was considered as at ground potential. When the boundary conditions of the model were defined, the model geometry was divided into the finite number of triangle elements by meshing as shown in Figure 3.

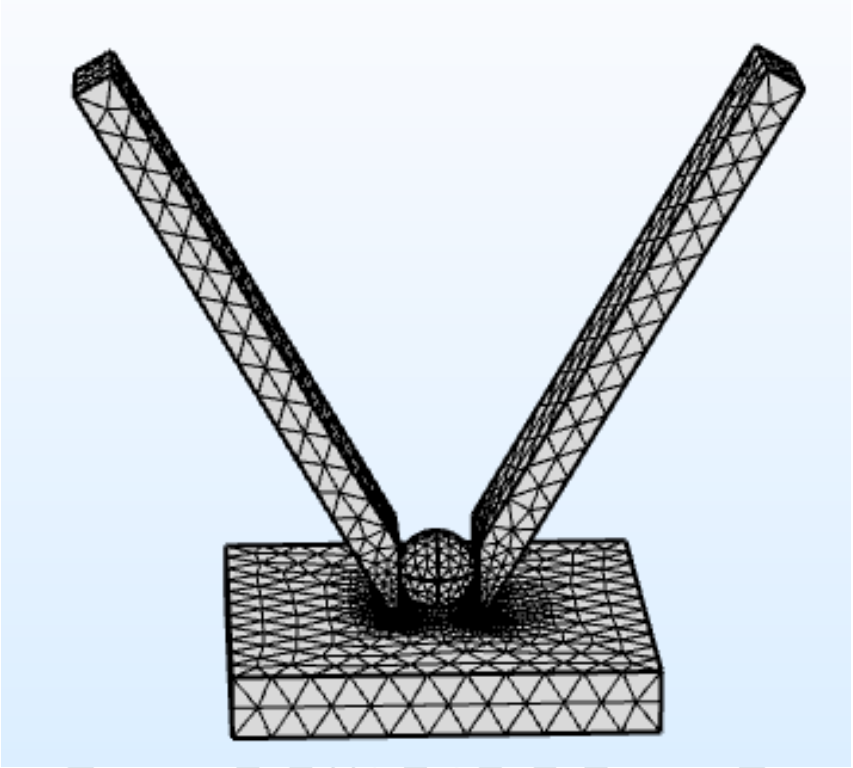

Figure 3: Meshing of Geometry

The CTI experiment was simulated by solving the following equations:

$$\nabla \times J = Q_j \quad (2)$$

$$J = \sigma E + J_e \quad (3)$$

$$E = -\nabla V \quad (4)$$

In these equations, ∇ is the differential operator; V is applied voltage (V); E is electric field intensity (V/m); J is the current density (A/m^2); Q_j is current source (A/m^3); Je is external current density (A/m^2); σ is electric conductivity (S/m). Q_j and J_e values in the solution of the problem are set to zero since no external current source is present.

To analyze the distribution of the electric potential and electric field on the polymer surface, the effects of a water droplet being dropped on the surface of a silicon rubber sample from the initial drop to the dispersion between electrodes were simulated.

III. Results and Discussion

3.1 Experimental Analysis

The test setup depicted in Figure 1 was utilized to conduct the CTI studies on SR samples. It was tested at three distinct test voltages: 200 V with 50 droplets, 175 V with 100 droplets, and 150 V with 200 droplets. The inter-electrode resistance considerably decreased during the test when a droplet of the solution slammed into the surface of the insulating substance being tested. This resulted in the flow of current, which heated up the conducting film between the electrodes and caused some of the solution to evaporate. The burn-in of specific patterns between two electrodes was the first visual event during the test method that was noticed. After 30-35 most recent drops, deep and notable burn-in patterns appeared and demonstrated a change in the surface structure of the sample being tested. Figure 4 displays the samples' post-test surface states.

Figure 4(a) and (b) show virgin and aged samples after CTI test respectively with 200 V, 50 drops, Fig. 4(c) and (d) show virgin and aged samples respectively with 175 V, 100 drops, and Fig. 4(e) and (f) show virgin and aged samples respectively with 175 V, 200 drops. In the figure, solid and dotted marks indicate the positions of HV and ground electrodes respectively. The figure shows that, even when the test voltage is decreased, the surface deterioration increases as the number of droplets increases. This is due to the sample's surface's higher conductivity, which is caused by the presence of more droplets. Additionally, in all three test circumstances, the aged samples show higher degradation than the fresh material. The burn-in patterns show that the sparks, which were local and happened in the middle of the electrodes, also caused flashovers that extended beyond the length of the electrodes. If such operating conditions occur in the power transmission network, the constant arcing on the insulator's surface may cause a sizable amount of mass erosion, which could reduce the insulator's mechanical strength.

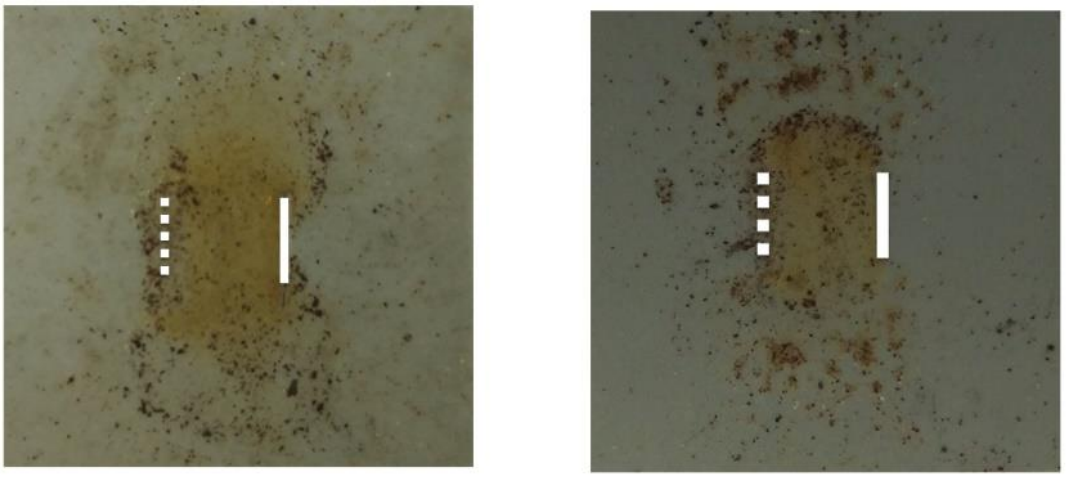

(a) Virgin Material (b) Aged Material

200 V, 50 Drops

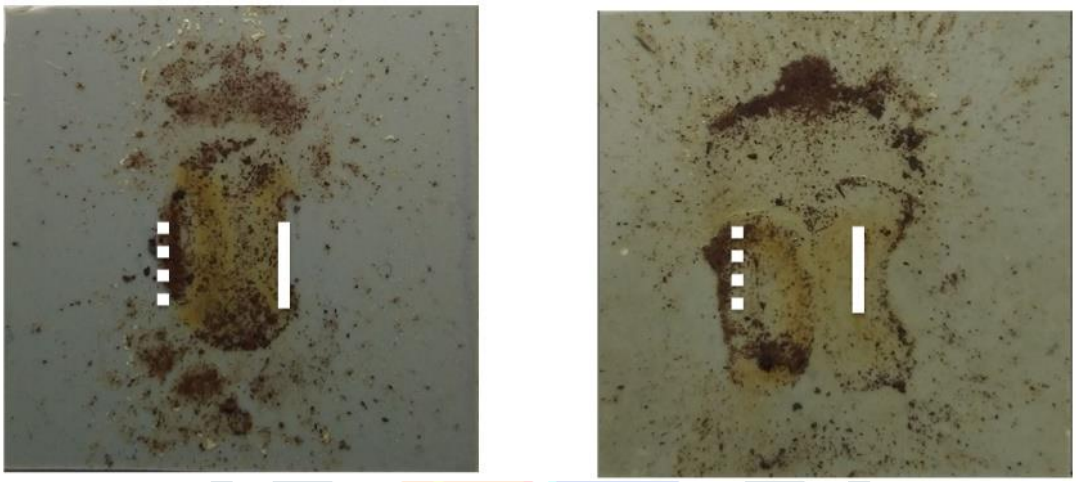

(c) Virgin Material (d) Aged Material

175 V, 100 Drops

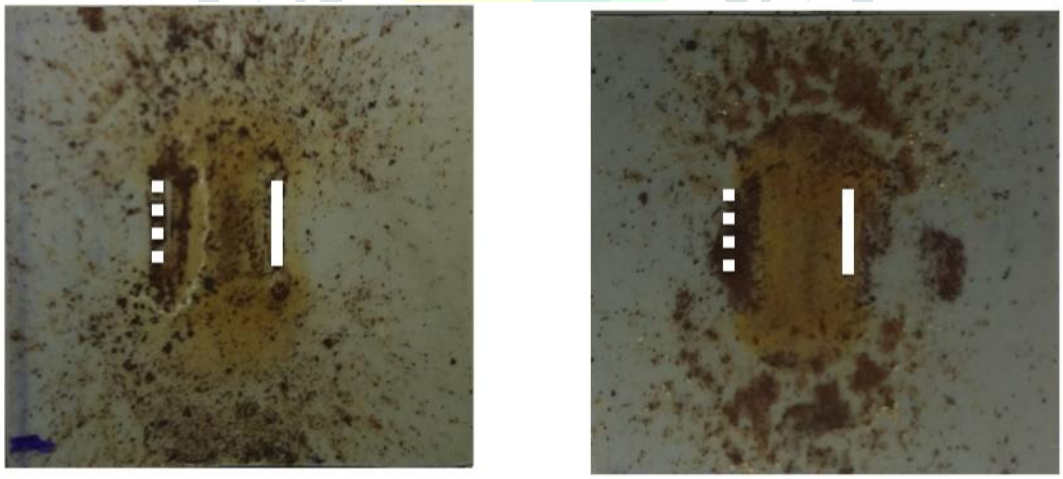

(e) Virgin Material (f) Aged Material

150 V, 200 Drops

Figure 4: Surface Condition of Tested Samples

With the use of the edge detection technique, the surface conditions of the samples were examined, and it was determined that the presence of edges on the surface indicated irregular surface conditions brought on by mass erosion brought on by electrical stress. Surface erosion increases as the number of edges increases. The images after the Sobel mask filter's edge detection are shown in Figure 5 so that the number of edges can be estimated.

For edge detection, which represents the points in the image with discontinuities, the mask filters Sobel and Prewitt were utilized. In Figure 6, the edge count is displayed. It is evident that aged samples have more edges than virgin samples. As a result of the current conduction on the samples' surfaces, it means that surface degradation is worse for older samples. Furthermore, despite lower potential, the surface condition deteriorates in both the samples with 200 droplets as opposed to 50 and 100 droplets.

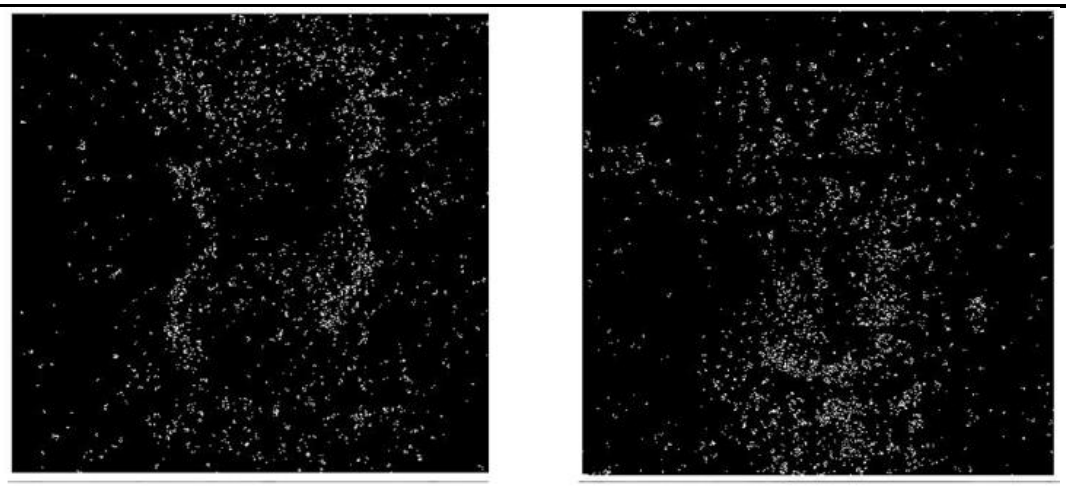

(a) Virgin Material (b) Aged Material

200 V, 50 Drops

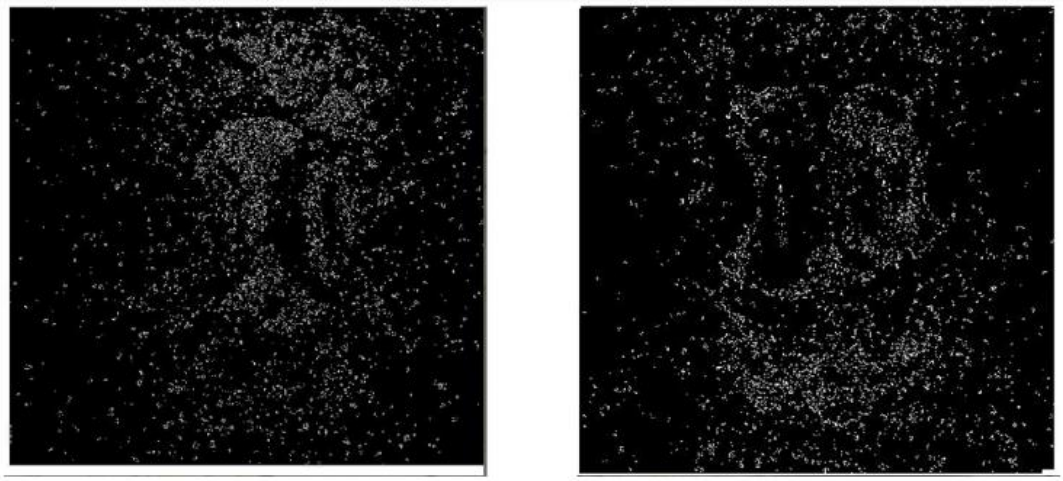

(c) Virgin Material (d) Aged Material

175 V, 100 Drops

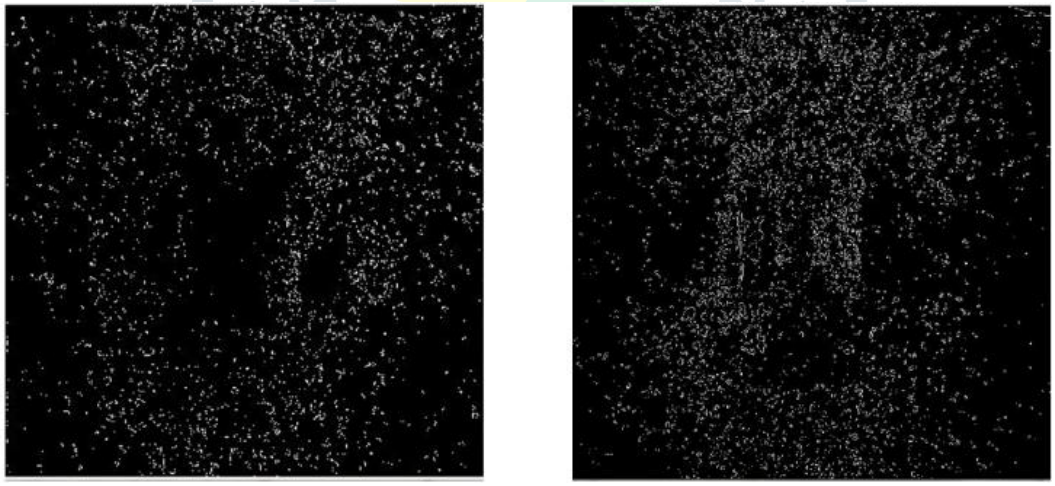

(e) Virgin Material (f) Aged Material

150 V, 200 Drops

Figure 5: Images of Tested Samples after Edge Detection with Sobel Filter

The simulation results presented below have a correlation with the edge detection results. The enhanced electric field created by the contaminant droplets between the electrodes causes more frequent arcing on the samples' surfaces, which led to material deterioration as evidenced by the increased number of edges. It is evident from the edge count that as the number of droplets increases, so does the edge count.

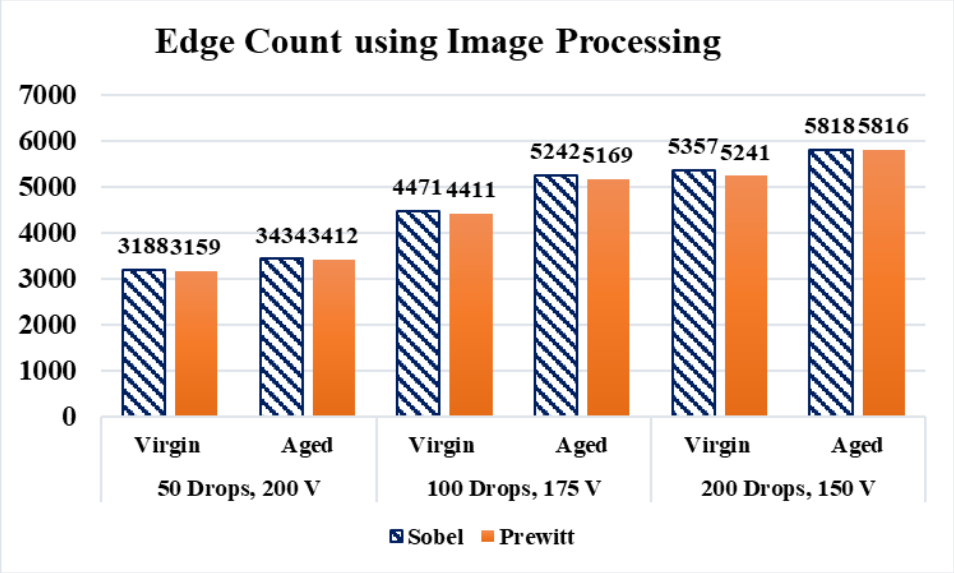

Figure 6: Edge Count with Sobel and Prewitt Filters

3.2 Simulation of CTI Test

The CTI test has been simulated under a variety of circumstances. Without and with water droplets, the electrical potential and electric field distribution between the electrodes have been plotted. The distribution of the electric potential and field between the electrodes without water droplets is shown in Figures 7(a) and (b).

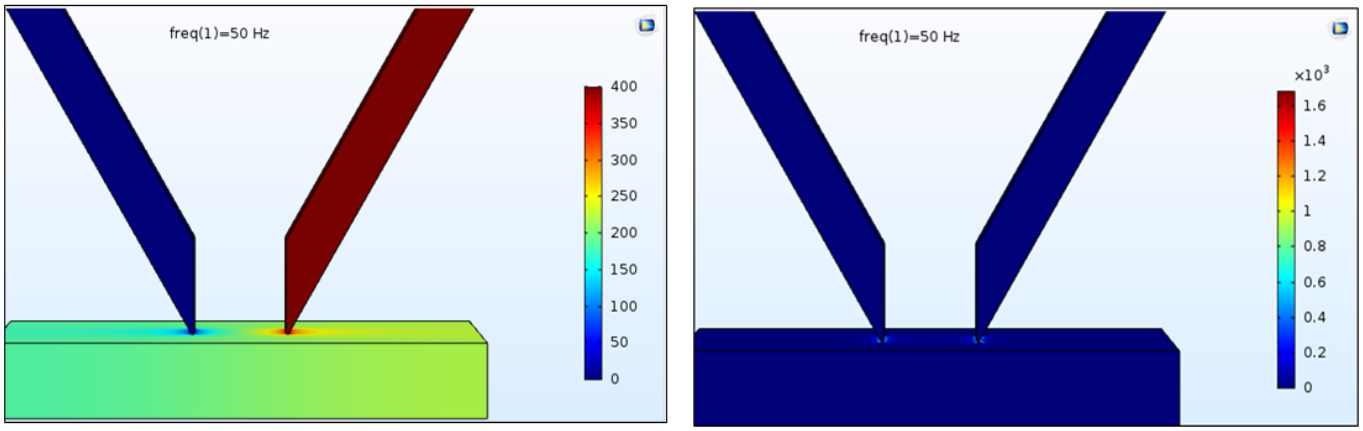

(a) (b)

Figure 7: (a) Electric Potential; (b) Electric Field Distribution without Droplet

The electric field intensity on the sample surface at 8 mm and 12 mm locations achieves the highest values at which the ground electrode and HV electrodes, respectively, touch the sample in the absence of the water droplet. The value of the electric field intensity between the electrodes is lower. A line is drawn through the center of the sample surface to track changes in the electric field there. This line extends from the ground electrode, starting at an HV electrode. From the center of the electrodes, this line extends. As seen in Figure 8, the variations in the electric field intensity are plotted on the graph for the whole length of the line. At the ground and HV electrodes, the maximum electric fields are found to be 1 kV/mm and 1.1 kV/mm, respectively.

As shown in Figure 9, a sphere droplet with a radius of 1.9134 mm is maintained at a height of 1 m above the sample surface to study how the pollutant affects the distribution of the electric field and potential energy. The electric field distribution is slightly altered as illustrated in Figure 10 because the water droplet's permittivity is different from the air between the electrodes. 1.25 kV/mm is observed to be the maximum field value at the HV electrode-sample interface.

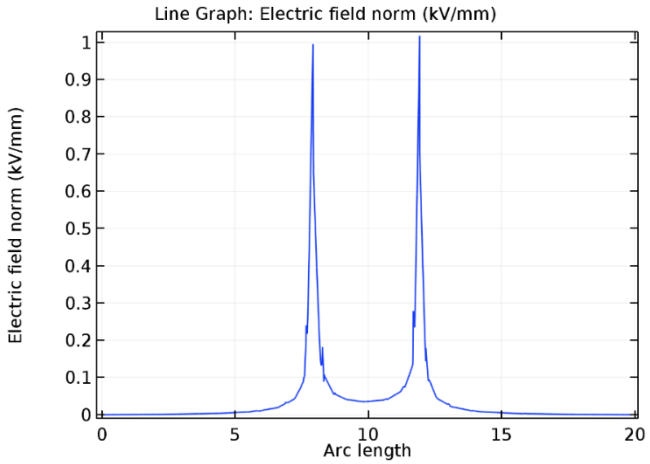

Figure 8: Electric Field Change between Electrodes without Droplet

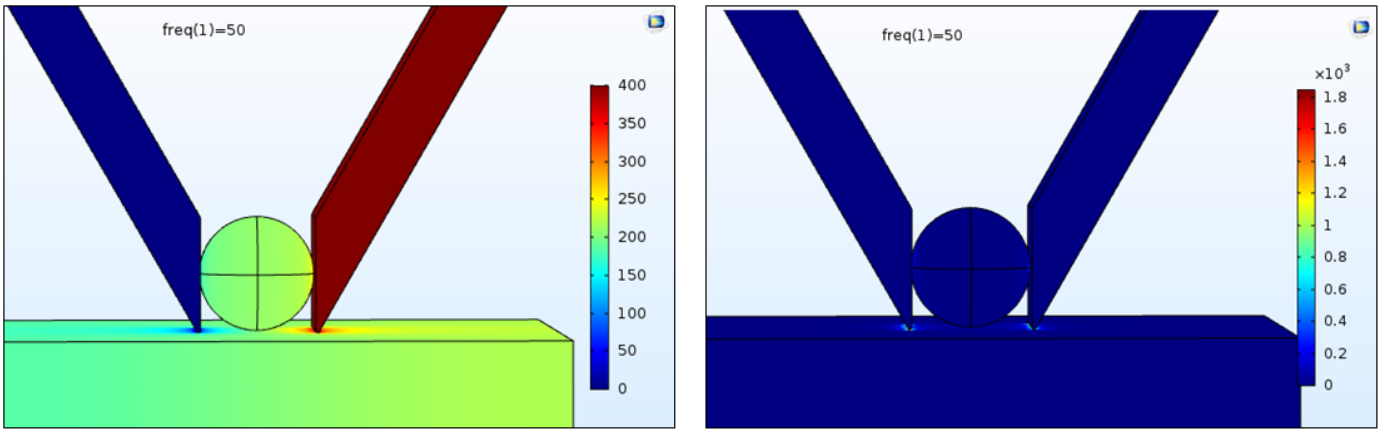

Figure 9: (a) Electric Potential; (b) Electric Field Distribution with Droplet

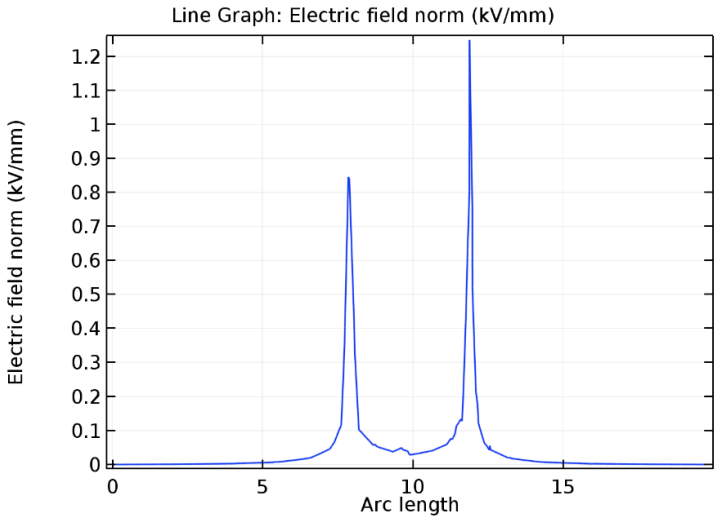

Figure 10: Electric Field Change between Electrodes with Droplet

When the droplet begins to spread across the sample's surface, as seen in Figure 11, the simulation is run. A strong electric field is created when the semi-spherical droplet hits or shorts both electrodes, as seen in Figure 12. In this instance, it is discovered that the field is roughly 1.65 kV/mm close to the HV electrode and 1.35 kV/mm close to the ground electrode.

The droplet is deemed to have nearly evaporated at this point. In this instance, it is producing an incredibly thin film on the sample's surface. When the droplet begins to evaporate, it has been found that the electric field is slightly diminished. As was previously noted, the application of electric potential in the presence of a contaminant on the surface of silicon rubber causes dry-band arcing, which leaves tracks on the surface and produces carbonaceous routes, both of which cause the surface to degrade Repeating the process causes the sample's surface to heat up, which causes mass erosion and weakens the material. The presence of water droplets also increases the electric field between the electrodes during the simulation of the CTI test, which results in electric stress on the surface and is one of the factors contributing to material deterioration.

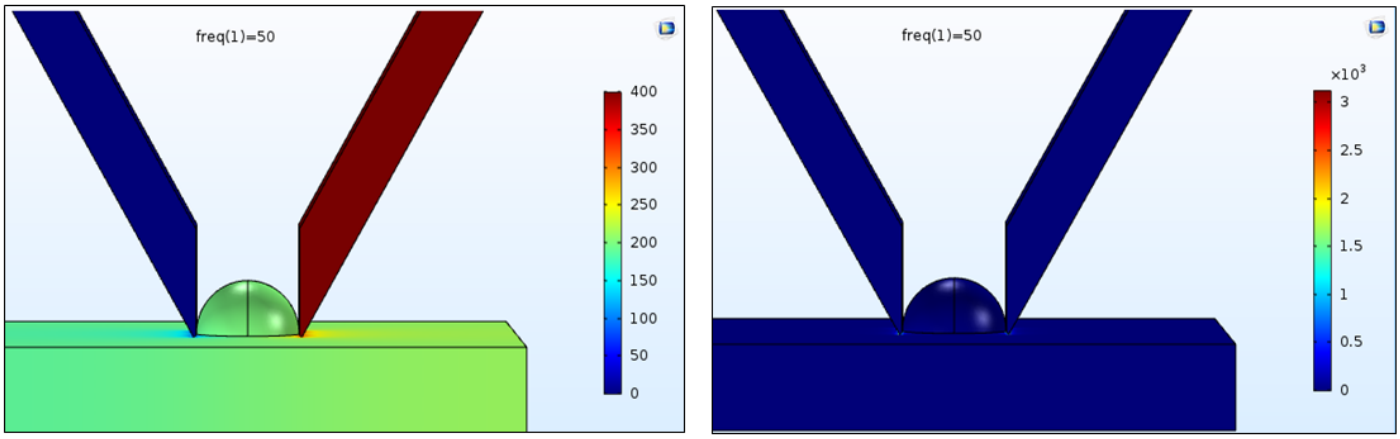

(a) (b)

Figure 11: (a) Electric Potential; (b) Electric Field Distribution with Semi-spherical Droplet

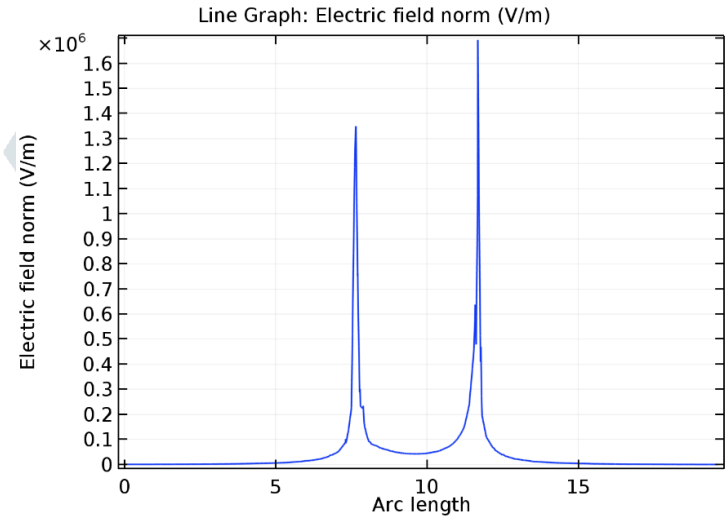

Figure 12: Electric Field Change between Electrodes with Semi-spherical Droplet

IV. CONCLUSIONS

With the help of CTI experiment on silicon rubber insulator and simulation of the same, it is concluded that

1) The presence of the pollutant significantly alters the surface characteristics, leading to mass erosion brought on by dry band arcing and the production of heat as the conductivity of the insulating material surface increases.
2) Using the Sobel algorithm with 150 volts and 200 droplets, the number of edges in the virgin sample is 5387, and in the aged sample, it is 5818. This demonstrates that older samples had greater tracking and deterioration than younger samples. All experimental instances yield the same outcomes.
3) Simulations confirm experimental findings that the presence of water droplets between the electrodes raises the electric field by 39%, which can result in electrical stresses on the surface of the material.

REFERENCES

[1] R S Gorur, E A Cherney and J.T. Burnham, 1999, Outdoor Insulators, Ravi S. Gorur Inc.
[2] K O Papailiou, F Schmuck, 2013. Silicone Composite Insulators- Materials, Design, Applications. Springer publications.
[3] J F Hall, 1993. History and bibliography of polymeric insulators for outdoor applications. IEEE Trans. Power Delivery. 8(1):376-385.
[4] Verma Alok Ranjan and Subba Reddy B., 2019. Interpretation of Surface Degradation. Engg. Failure Analysis, 95:214-225.
[5] Yoshimura N, Nishida M, Noto F. 1981. Influence of the electrolyte on tracking breakdown of organic insulating materials. IEEE Trans Electr. Insul., 16(6):510–520.
[6] L Centurioni, G Coletti, A Operato., 1977. A contribution to the study of the tracking phenomenon in solid dielectric insulating materials under moist conditions. IEEE Trans. Electr. Insul., 12(2):147- 152.
[7] IEC 60112. 2003. Determining of the comparative and proof tracking indices of solid insulating materials under moist conditions.

[8] K Kawamura, S Sakamoto., 1982. Processes contributing to low DC tracking failure. IEEE Trans. Electr. Insul., 17(3):241-247.

[9] B X Du. 2001. Discharge Energy and DC Tracking Resistance of Organic Insulating Materials. IEEE Trans. Dielectr. Electr. Insul., 8:897-901.

[10] B X Du, L Gu, D S Dongand, X L Zheng. 2008. Recurrent plot analysis of discharge sequences in tracking test of polybutylene polymers. J. Phys. Appl. Phys., 41. 195412 (7 pp).

[11] B X Du, H J Liu. 2009. The Application of Recurrence Plot in DC Tracking Test of Gamma-ray Irradiated Polycarbonate. IEEE Trans. Dielectr. Electr. Insul., 16(1):17-23.

[12] Subba Reddy B and Rajalingam M. 2016. Recurrence Plot Analysis to Estimate the Surface Erosion on Polymeric Insulating Materials. IEEE Trans. Electr. Insul., 23(3):1620- 1626.

[13] Ispirli M M, Ersoy Yilmaz A, Kalenderli O. 2018. Investigation of tracking phenomenon in cable joints as 3D with finite element method. Electr. Eng., 100:2193–2203.

[14] A Fuchs, H Zangl. 2008. Observations and Restrictions for Tracking Indices Measurement in Materials Testing. International Journal on Smart Sensing and Intelligent Systems., 1(3):623-637.

[15] Xing Z, Zhang C, Hu X, Guo P, Zhang J, Wang Z, Wu K, Li J. 2019. Surface Tracking of MgO/Epoxy Nanocomposites: Effect of Surface Hydrophobicity. Appl. Sciences., 9(3):413**.**

[16] IEC Publ. 60112:1979 Method for determining the comparative and the proof tracking indices of solid insulating material under moist conditions, 3rd edn.

[17] G E Rani, R Murugeswari, N Rajini. 2020. Edge Detection in Scanning Electron Microscope (SEM) Images using Various Algorithms. Proceedings of the International Conference on Intelligent Computing and Control Systems (ICICCS 2020). IEEE Xplore Part Number: CFP20K74-ART; ISBN: 978-1-7281-4876-2.

[18] Pinaki Pratim Acharjya, Ritaban Das, Dibyendu Ghoshal. 2012. Study and Comparison of Different Edge Detectors for Image Segmentation. Global Journal of Computer Science and Technology Graphics & Vision., 12(13).

[19] COMSOL Multiphysics v. 5.2. (2015) COMSOL AB, Stockholm, Sweden. http://comsol.com. Accessed 10 May 2017.